ELSEVIER

Contents lists available at ScienceDirect

Neurobiology of Learning and Memory

journal homepage: www.elsevier.com/locate/ynlme



Coupling of autonomic and central events during sleep benefits declarative memory consolidation



Mohsen Naji^a, Giri P. Krishnan^a, Elizabeth A. McDevitt^b, Maxim Bazhenov^a, Sara C. Mednick^{c,*}

- ^a Department of Medicine, University of California San Diego, La Jolla, CA, USA
- ^b Princeton Neuroscience Institute, Princeton University, Princeton, NJ, USA
- ^c Department of Cognitive Sciences, University of California Irvine, Irvine, CA, USA

ABSTRACT

While anatomical pathways between forebrain cognitive and brainstem autonomic nervous centers are well-defined, autonomic—central interactions during sleep and their contribution to waking performance are not understood. Here, we analyzed simultaneous central activity via electroencephalography (EEG) and autonomic heart beat-to-beat intervals (RR intervals) from electrocardiography (ECG) during wake and daytime sleep. We identified bursts of ECG activity that lasted 4–5 s and predominated in non-rapid-eye-movement sleep (NREM). Using event-based analysis of NREM sleep, we found an increase in delta (0.5–4 Hz) and sigma (12–15 Hz) power and an elevated density of slow oscillations (0.5–1 Hz) about 5 s prior to peak of the heart rate burst, as well as a surge in vagal activity, assessed by high-frequency (HF) component of RR intervals. Using regression framework, we show that these Autonomic/Central Events (ACE) positively predicted post-nap improvement in a declarative memory task after controlling for the effects of spindles and slow oscillations from sleep periods without ACE. No such relation was found between memory performance and a control nap. Additionally, NREM ACE negatively correlated with REM sleep and learning in a non-declarative memory task. These results provide the first evidence that coordinated autonomic and central events play a significant role in declarative memory consolidation.

1. Introduction

It is now well-established that specific electrophysiological central events during sleep support the transformation of recent experiences into long-term memories, i.e., memory consolidation. Another direction of research has demonstrated evidence for a critical role of autonomic activity during waking in memory and learning. We have recently shown that autonomic activity during sleep may also be related to consolidation. What is not known is whether the coupling of central and autonomic systems during wake or sleep plays a role in memory consolidation. Here, we identify a novel coupling between the autonomic and central nervous systems during sleep, but not wake, that predicts the outcome of the memory consolidation.

Research has consistently shown that a period of non-rapid eye movement (NREM) sleep yields greater memory retention of declarative memories (e.g., explicit, episodic memories) than a comparable period of rapid eye movement (REM) sleep or waking activity (Gais & Born, 2004). Several EEG features of NREM sleep have been linked with memory consolidation, with most studies focusing on spectral power in the slow wave activity (0.5–4 Hz) and sigma (12–15 Hz) bands, or specific events including hippocampal sharp wave-ripples (~150–250 Hz), cortical slow oscillations (SO, ~0.5–1 Hz), and thalamic sleep spindles (~12–15 Hz). In fact, co-occurring SOs and sigma/spindles may be a key mechanism of memory consolidation during

In humans, increases in sigma power during the SO up-states has been shown following learning of a declarative memory task (Mölle, Eschenko, Gais, Sara, & Born, 2009). Furthermore, pharmacologically increasing spindles with zolpidem resulted in greater coupling of spindles and SOs (Niknazar, Krishnan, Bazhenov, & Mednick, 2015) and declarative memory improvements (Mednick et al., 2013); (also see (Arbon, Knurowska, & Dijk, 2015) (Hall et al., 2014)). In rodents, the replay of neural activity from encoding during sleep has been proposed to occur through the temporal coupling of thalamic spindles, hippocampal sharp wave ripples, and cortical slow oscillations (Staresina et al., 2015). Thus, although a full mechanistic understanding of sleep-dependent memory consolidation is far from realized, research suggests that the coordination of brain rhythms from several cortical and subcortical regions may be critical.

A different line of research has demonstrated a significant contribution of the autonomic nervous system for memory consolidation during waking (McGaugh, 2013). These studies implicate the tenth cranial "vagus" nerve as the primary pathway of communication between the autonomic and central nervous systems. The vagus communicates information about peripheral excitation and arousal via projections to the brainstem, which then project to many memory-related brain areas, including the amygdala complex, hippocampus and prefrontal cortex (PFC) (Packard, Williams, Cahill, & McGaugh, 1995).

E-mail address: mednicks@uci.edu (S.C. Mednick).

sleep (Staresina et al., 2015).

^{*} Corresponding author.

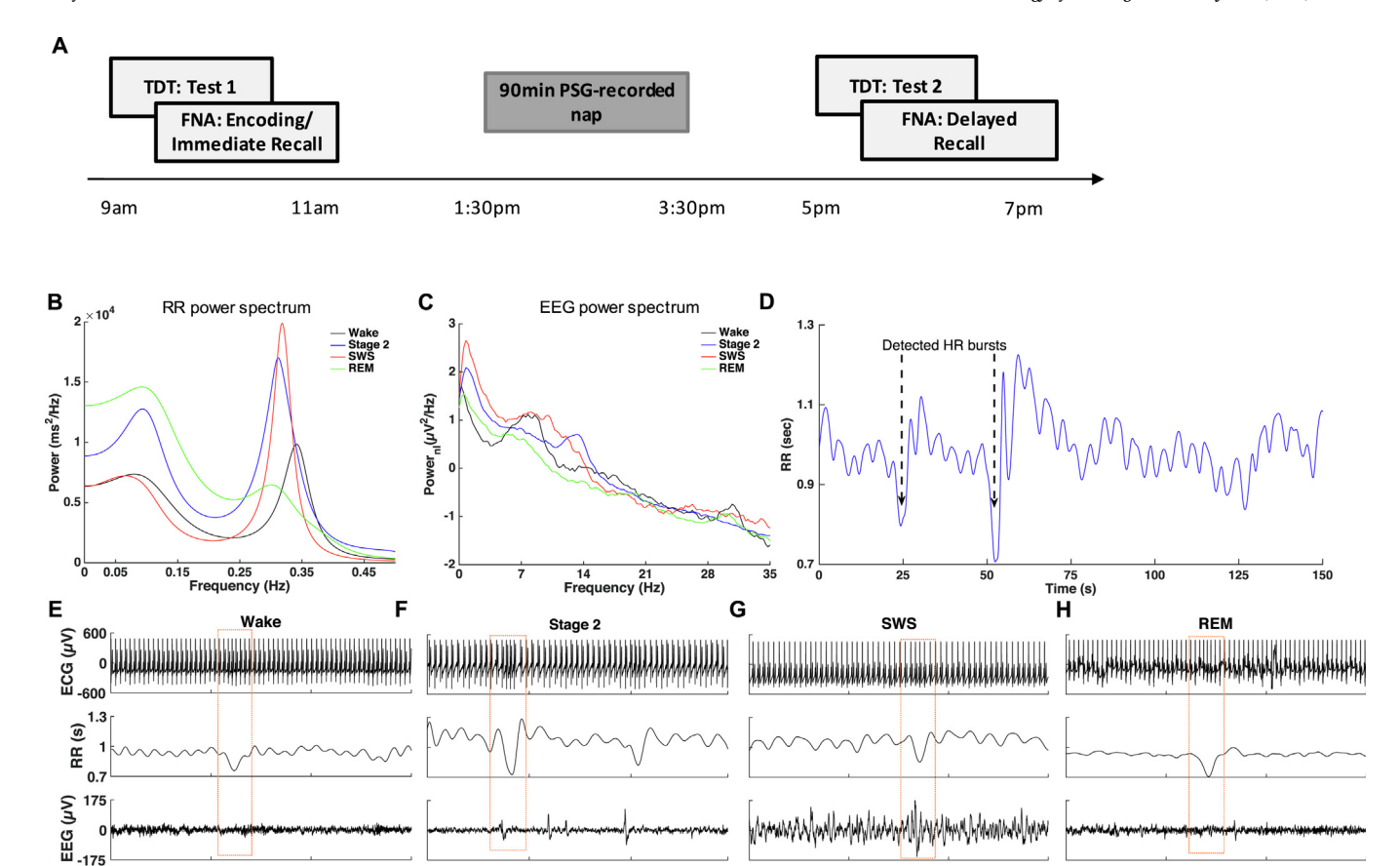


Fig. 1. Study timeline and characteristic properties of the EEG and RR time-series signals across wake and sleep stages (for one participant). (A) Subjects completed two memory tasks: a declarative face-name association (FNA) task and a non-declarative texture discrimination task (TDT). The order of tasks was counterbalanced across subjects. Before and after the daytime nap, declarative and non-declarative memory performance was tested. (B) RR time-series power spectrum during wake and sleep stages. (C) EEG power spectrum (0–35 Hz) during wake and sleep stages. (D) Detected heart rate bursts within a 150-s bin during Stage 2. (E–H) Simultaneous presentation of ECG, RR time-series, and raw EEG within 60-s windows during wake, Stage 2, SWS, and REM, respectively. The boxes show the coincidence of heart rate bursts and EEG events during Stage 2 and SWS.

Descending projections from the PFC to autonomic/visceral sites of the hypothalamus and brainstem create a feedback loop allowing for bidirectional communication between central memory areas and peripheral sites (Thayer & Lane, 2009). In male sprague-dawley rats, postencoding vagotomy impairs memory (Williams & Jensen, 1993). In humans, vagal nerve stimulation during verbal memory consolidation enhances recognition memory (Clark, Naritoku, Smith, Browning, & Jensen, 1999). Thus, the autonomic nervous system (ANS) appears to play a substantial role in waking memory consolidation.

We have recently shown that ANS activity during REM sleep is also associated with memory consolidation (Whitehurst, Cellini, McDevitt, Duggan, & Mednick, 2016). In this study, subjects were given a memory test before and after a daytime nap. Along with measuring central activity during sleep, we also measured ANS activity using the traditional approach of heart rate variability (HRV), defined as the variance between consecutive heartbeats averaged within each sleep stage, as well as during a pre-nap wake period. We found that vagally-mediated ANS activity during sleep (1) is associated with the consolidation of implicit and explicit information, and (2) is sleep stage specific.

Given the evidence of independent contributions of central and autonomic activity during sleep for memory consolidation, it is not known whether there is coupling between these systems and whether this coupling may support long-term memory formation. Prior work hints at a possible coordination between central features and autonomic activity. For example, auditory-evoked K-complexes were associated with increased heart rate (de Zambotti et al., 2016) and have been shown to appear frequently 250 and 650 ms after the onset of the P

wave in the electrocardiogram (ECG) (Fruhistorfer, Partanen, & Lumio, 1971). Furthermore, the QRS complex of ECG has been shown to modulate sleep spindle phases (Lechinger, Heib, Gruber, Schabus, & Klimesch, 2015). In addition, the high frequency component of HRV, which reflects parasympathetic activity, has been shown to correlate with slow wave activity in the brain (Brandenberger, Ehrhart, Piquard, & Simon, 2001). Finally, volitional effort during wake correlates both with increases in hippocampal activity and heart rate (Norton, Luchyshyn, & Shoemaker, 2013); and phase-locking between central hippocampal theta and autonomic R-waves has been shown in guinea pigs during wake, slow wave sleep (SWS) and REM sleep (Pedemonte, Goldstein-Daruech, & Velluti, 2003). Together, these findings suggest that cardiac autonomic activity may be coupled with hippocampothalamocortical communication that has been shown to underlie memory consolidation during sleep. Despite these intriguing associations, very little is known about the coupling of central and autonomic activity and its functional consequences.

Here, we used a high-temporal precision time-series approach to examine coupling between central and autonomic nervous system activity during wake and sleep and its impact on memory consolidation. Using this approach, we identified novel cardiovascular events during NREM sleep, heart rate bursts, which are temporally coincident with increases in electrophysiological central events that have previously been shown to be critical for sleep-dependent memory consolidation. In addition, these Autonomic/Central Coupled Events (ACE) are directly following by a surge in vagal activity, indexed by the high-frequency component of RR intervals. Using a regression framework, we assessed

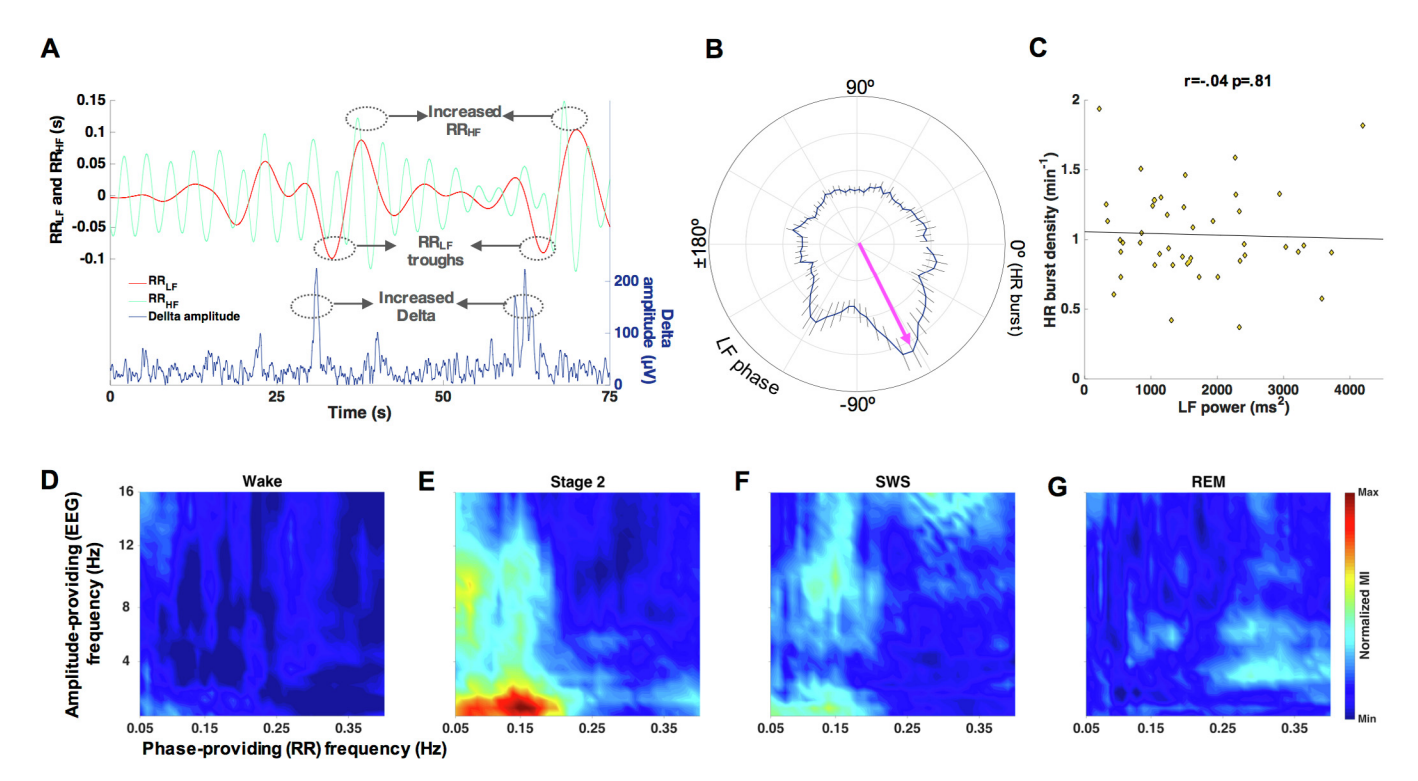


Fig. 2. Temporal analysis of the RR intervals. (A) A simultaneous presentation of delta amplitude and filtered components of RR time-series (i.e., LF and HF) showing the coincidence of large troughs in the LF component and elevated delta amplitude. (B) The distribution of delta amplitude in LF phase is non-uniform and peaks at a preferred phase (LF troughs are assigned phase 0). (C) The density of heart rate bursts does not significantly affect the LF power. (D–G) The average EEG/ECG comodulograms, constructed from RR phase and EEG amplitude, across participants during wake, Stage 2, SWS, and REM, respectively. Error bars show standard error of the mean.

the contribution of ACE events versus non-ACE central and autonomic activity to declarative memory improvement following a nap, and show that ACE events predict performance improvement to a greater extent than by either activity alone. No such relation was found between memory performance and a control nap. We, thus, demonstrate a heretofore-unrecognized important role of coordinated autonomic and central activity during sleep that supports declarative memory consolidation.

2. Results

We analyzed the RR (inter-beat interval) time-series from the ECG, and electrical brain activity from frontal and central EEG recording sites, during a daytime nap in 45 young, healthy subjects (see Fig. 1A for Study Timeline). First, we assessed ANS activity using the traditional method of analyzing heart rate in the frequency domain - heart rate variability (HRV). In the frequency domain, the low frequency (LF; 0.04-0.15 Hz) component of RR is considered a reflection of sympathetic nervous activity (Malik et al., 1996) (although this is not universally accepted (Billman, 2013)), while the high frequency (HF; 0.15–0.4 Hz) component reflects parasympathetic (vagal) activity (Malik et al., 1996). Prior studies have demonstrated a decrease in LF and an increase in HF components in NREM during nighttime sleep (Vanoli et al., 1995) and naps (Cellini, Whitehurst, McDevitt, & Mednick, 2016). In agreement with this literature, we found that the power spectrum of the RR time-series was modulated by sleep stages (Fig. 1B). Furthermore, different sleep stages showed distinct properties in the EEG frequency-domain. Peaks emerged in delta (0.5-4 Hz), theta (4-8 Hz), alpha (8-13 Hz), and sigma (12-15 Hz) bandwidth of EEG power spectrum (Fig. 1C).

We also employed a time-domain analysis approach to the ECG signal to investigate the events that last for few seconds and might be neglected by classic HRV analyses in 3–5 min epochs. After confirming

the detected ECG R peaks by visual inspection, we intentionally analyzed all artifact-free RR intervals without rejecting RR intervals that were too short or too long (a common practice in traditional HRV studies (Malik et al., 1996)), thereby retaining a larger amount of RR intervals than typical for HR analysis. Using this approach, we observed large bursts in heart rate (i.e., decreased RR intervals) over periods of 4–5 s (Fig. 1D). Further, these heart rate (HR) bursts were visually noted to co-occur with events in the EEG (see boxes in Fig. 1E–H). In the next section we provide a detailed analysis of these heart rate bursts and their coincidence with events in the EEG.

2.1. Temporal analysis of RR intervals reveals distinct, intermittent reductions in RR intervals

The heart rate bursts sporadically emerged in the time series of RR intervals (Fig. 1D). The signature of these heart rate bursts was an increase in HR from baseline to the peak of the heart rate bursts (Wake: 21.62% (s.d. = 11.05); Stage 2: 20.69% (s.d. = 7.53); SWS: 14.49% (s.d. = 6.02); REM: 21.40% (s.d. = 8.85)). The densities of the heart rate bursts for Wake, Stage 2, SWS, and REM were 0.71 per minute (s.d. = 0.52), 1.04 per minute (s.d. = 0.32), 1.11 per minute (s.d. = 0.34), and 1.00 per minute (s.d. = 0.38), respectively. Shapiro-Wilk and Chi-square tests on inter-event-intervals revealed that these events are generally aperiodic (Fig. S1).

Following the visual observation of the co-occurrence of heart rate bursts and EEG events we assessed the degree to which the heart rate bursts correlated with changes in EEG activity (Fig. 1E–H). We found that EEG delta amplitude during heart rate bursts was significantly higher than during non-bursting periods of the RR signal in both Stage 2 (t(84) = 2.14, p = .035)) and SWS (t(70) = 1.70, p = .046), but not Wake (t(62) = 1.14, p = .257) and REM (t(56) = 0.38, p = .706). Traditional measures of HR in the frequency domain examine LF and HF power by collapsing across time. However, given our interest in

moment-to-moment changes in ANS/CNS signals, we filtered the RR time-series by LF and HF frequency bands (RR_{LF} and RR_{HF}, respectively), thereby maintaining the integrity of the time-series data. Similarly, we filtered the EEG time-series within the delta frequency to analyze the dynamics of the ANS/CNS interaction. We noted that during Stage 2 and SWS, bursts in delta amplitude co-occurred with large troughs in RR_{LF} (corresponding to heart rate bursts), which were followed by increases in RR_{HF} (see an example in Fig. 2A). We further investigated this coincidence by examining the the phase/amplitude coupling (PAC) between delta and RR_{LF}, where the slow frequency RR_{LF} provides the phase and the faster frequency delta provides the amplitude. During Stage 2 and SWS, the distribution of delta amplitude in the LF phase was non-uniform and peaked at a preferred phase (Fig. 2B). the average preferred participants, -70.1° (s.d. = 26.7°) for Stage 2 and -79.4° (s.d. = 67.6°) for SWS. This also indicates that the elevation in EEG delta activity preceded the peak of the Heart rate bursts (which occurred at LF phase of 0°). Interestingly, when we compared the density of the heart rate bursts to the traditional FFT analysis of LF power (i.e., likely sympathetic activity) within Stage 2 and SWS, total LF power was not significantly associated with heart rate burst density in Stage 2 (r = -0.04, p = .81; Fig. 2C) or SWS (r = -0.08, p = .64). We next set out to investigate the PAC between EEG and RR across a broader frequency range.

2.2. EEG power is modulated by RR phase

We used the comodulogram method, utilizing normalized modulation index (nMI) as the PAC measure, to examine how the fast EEG signal was nested within the slower RR time-series signal across Wake, Stage 2, SWS and REM sleep. Conceptually, for each frequency pair in the comodulograms the modulation of EEG amplitude by RR phase was compared to amplitude-shuffled surrogate data. Fig. 2E shows the phase of the RR time-series in frequencies below 0.2 Hz strongly modulated the amplitude in EEG in frequencies below 4 Hz, slow wave activity (SWA), during Stage 2. The same relation was apparent for SWS, but to a lesser extent (unpaired t-test between LF-SWA nMI of Stage 2 and SWS: (t(77) = 3.21, p = .002) (Fig. 2F). The LF-SWA modulation during Stage 2 and SWS was significantly higher than that of other RR/ EEG frequency pairs (i.e., LF-theta, LF-alpha, LF-sigma, HF-SWA, HF-theta, HF-alpha, and HF-sigma; Stage 2: $F_{7.336} = 5.83$, p = .000002; SWS: $F_{7,280}$ = 2.97, p = .005). Taken together, the time series analysis indicates that EEG SWA amplitude in Stage 2 and SWS was modulated by the LF component of the RR time-series (RR_{LF}).

Though LF-SWA modulation was the strongest effect observed, the comodulogram also revealed other bands of EEG (< 16 Hz) that were modulated by LF phase in Stage 2 compared with Wake and other sleep stages (LF-SWA: $F_{3,145} = 10.44$, p = .00001; LF-theta: $F_{3,145} = 13.20$, p = .004;LF-alpha: $F_{3,145} = 17.58,$ p = .0005; $F_{3.145} = 13.93$, p = .003). For REM sleep (Fig. 2G), HF-modulated EEG theta activity was significantly higher than that of Wake (t(69) = 4.85,p = .000007) and SWS (t(66) = 2.06, p = .043) ($F_{2,103} = 7.34$, p = .002) but not Stage 2 (t(73) = 0.45, p = .65). The other clusters visualized by the SWS comodulograms were not significantly different from Wake and sleep stages. In the following section, we will test the hypothesis that the above-mentioned modulation results from temporal coupling of autonomic and central events (ACE).

2.3. Coordination between heart rate bursts and EEG

We investigated ACE coupling during wake and sleep stages by tracking fluctuations in the EEG in a 20-s window from 10 s before to 10 s after the peak of the Heart rate burst (Fig. 3A–B). In addition to the rapid acceleration in HR, we also noted a slowing of HR after the burst or peak of the HR. We chose to use the peak of the Heart rate burst as reference points because we found a larger number of heart rate bursts compared to HR troughs. The percentage of heart rate bursts which

were followed by HR declines was $12.61 \pm 2.71\%$ during Wake, $20.30 \pm 2.14\%$ during Stage 2, $13.30 \pm 2.65\%$ during SWS, and $27.02 \pm 4.00\%$ during REM. Therefore, the detection of the peaks was a more reliable metric of the heart rate bursts compared to detection of slower and smaller changes in HR. Furthermore, the magnitude of the HR slowing after the peak of HR was highly variable across heart rate bursts (see Fig. S2).

As we were specifically interested in EEG activity related to memory consolidation, we narrowed our frequencies of interest to SWA (and SOs) and sigma activity (and spindles). EEG data were binned into 5-s intervals within the 20-s windows around the Heart rate burst. Repeated measures ANOVAs indicated significant differences in SWA (Fig. 3E) across the 5-s bins and periods with no Heart rate burst (baseline) during Stage 2 ($F_{4,168} = 94.37$, p < .00001) as well as during SWS ($F_{4,140} = 21.59$, p < .00001). Post hoc comparisons revealed the highest SWA occurred during the 5-s bin prior to the Heart rate burst during Stage 2 (t(84) = 8.94, p < .00001) as well as during SWS (t(70) = 2.05, p = .044). Interestingly, the change in SWA in the 5-s bin prior to the heart rate bursts was significantly correlated with the increase in HF power in the 5-s bin after the Heart rate burst (Fig. 3C) during Stage 2 (r = 0.54, p = .002), likely reflecting a compensatory increase in vagal activity. This elevated increase in HF power after the Heart rate burst was also present during other sleep stages (Fig. 3C; Wake: t(44) = 1.78, p = .082; SWS: t(70) = 1.94, p = .056; REM: t(36) = 2.12, p = .041, nonsignificant after FDR correction). Similar to SWA, density in SOs in the 5-s bin prior to the Heart rate burst was significantly increased in Stage 2 (Fig. 3D, t(84) = 8.83, p < .00001) as well as during SWS (t(70) = 3.10, p = .007). Note that SWA without SO events (1-4 Hz, 33.25 \pm 2.88% of incidences) was also increased prior to the Heart rate burst (t(82) = 2.77, p = .003) during Stage 2. No significant correlation between heart rate bursts and SWA was found during Wake ($F_{3,112} = 1.41$, p = .24) or REM $(F_{3.116} = 0.24, p = .87)$. To summarize, we found that ACE in Stage 2 and SWS, but not wake and REM sleep, were characterized by an increase in EEG SWA that occurred 5-s before the peak of the Heart rate burst and ended simultaneously with the heart rate bursts.

Repeated measures ANOVAs also indicated significant differences in sigma activity (Fig. 3F) across the 5-s bins and periods with no Heart rate burst during Stage 2 ($F_{4.168} = 56.87$, p < .00001). The highest sigma power occurred during the 5-s bin prior the Heart rate burst (t (84) = 4.71, p = .00001). The early change in sigma power (10 s prior the peak of the Heart rate bursts) was not significant after FDR correction (t(84) = 1.90, p = .061; Fig. 3F). Similarly, repeated measure ANOVA indicated significant differences in spindle density across the 5s bins and periods with no Heart rate burst ($F_{4,168} = 2.93$, p = .022, Fig. S3). Post hoc paired-samples t-tests between baseline spindle density and the spindle density during the 5-s bins revealed a significant density difference during the 5-s bin prior the Heart rate burst peak (t (84) = 3.679, p = .0004) and a nonsignificant significant difference during the 5-s bin started 10 s before the Heart rate burst peak (t (84) = 1.871, p = .065). No significant modulation in sigma power was found during SWS (t(70) = 0.17, p = .86).

In addition to SWA and sigma activity, the coupling of SO and spindles as a function of the HR was investigated. For each subject, the average SO/spindle modulation index (Tort, Komorowski, Eichenbaum, & Kopell, 2010) was calculated for two groups of SOs: (1) SOs occurred during the 20-s windows around heart rate bursts and (2) SOs during periods with no Heart rate burst. Paired t-test showed no difference in MI for the two SO groups (t(87) = 0.177, p = .860). That is, ACE-related sleep activity did not have any measurable impact on the temporal coupling of SO and spindles.

In summary, Sigma and SWA power in Stage 2 and SWA in SWS increased from baseline (periods with no Heart rate burst) to a maximum level prior to the peak of the heart rate bursts, and returned to baseline post-burst. Although we focused on slow wave and sigma frequencies here, we conducted exploratory analyses on theta and beta

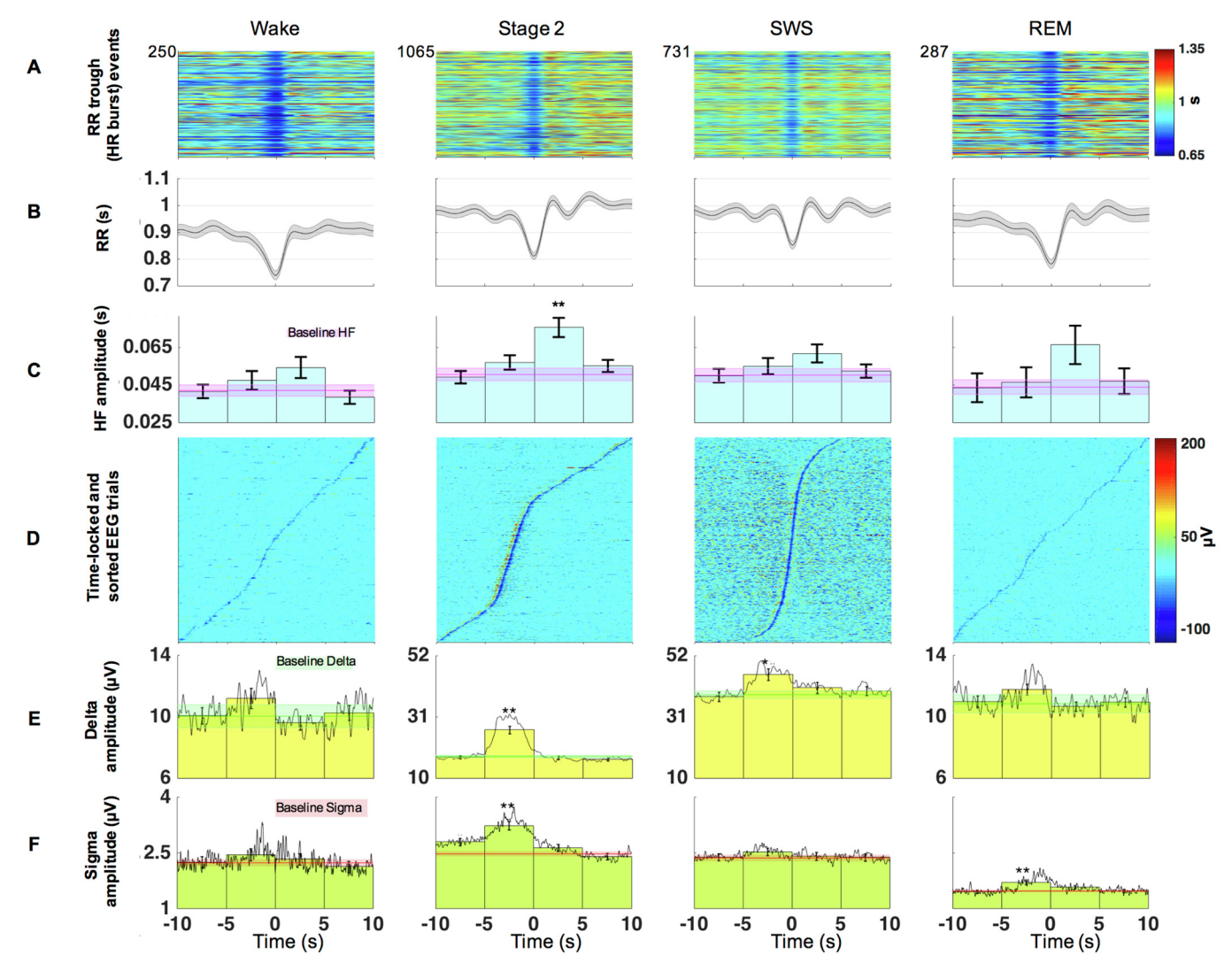


Fig. 3. The event-related analysis of changes in ACE events. (A) The Heart rate burst events within a 20 s window for wake and different sleep stages. (B) Grand average of the heart rate bursts. (C) Average amplitude of HF component of the heart rate bursts in 5-s bins show a significant increase in the 5-s bin after the peak of the heart rate bursts. (D) Event-locked EEG trials (Sorted based on the time difference between the Heart rate burst at t=0 and the largest minimum of the EEG trials) show concentration of SOs prior the peak of heart rate bursts in NREM stages. (E–F) average delta and sigma amplitude in 5-s bins (with the grand average of Delta amplitude on top of them) around the heart rate bursts, respectively. Asterisks in ϵ , (E), and (F) show the significant differences after FDR correction (*p < .05 and **p < .001) between an amplitude in a bin and the average amplitude in periods with no Heart rate burst (baseline). Error bars show standard error of the mean.

activity, which are presented in the Supplementary Materials. These data are consistent with the hypothesis that cortical EEG activity precedes and perhaps catalyzes these sudden and short-lived surges in HR in NREM sleep. We next investigated the functional impact of ACE events on memory consolidation during sleep.

2.4. Correlations with cognitive tasks

In this section, we investigated the contribution of ACE coupling to post-nap memory consolidation. For this purpose, we computed the change scores for both performance and EEG features coupled with ACE (i.e., ACE difference scores). The following EEG features were analyzed: density of SOs and magnitude of SWA and sigma power in Stage 2 and SWS, and a linear composite of SWA and sigma power changes (i.e., a simple sum of z-scores of SWA and sigma power changes) in Stage 2 (Fig. 4); we focused on Stage 2 and SWS, as ACE were not significantly modulated during wake or REM. ACE difference scores were calculated as average values of each EEG feature of interest 5 s prior to the peak of the heart rate bursts subtracted from baseline. We conducted exploratory analyses on the application of modulation index between

heart rate bursts and EEG activities, which are presented in the Supplementary Materials (see Fig. S5). Two memory tasks were considered for this study: declarative memory for face-name associations and non-declarative perceptual learning on a texture discrimination task. We calculated difference scores between pre-nap and post-nap memory performance for total (first and last name) recall and perceptual learning thresholds.

2.4.1. Declarative memory

Recall difference scores were positively correlated with ACE difference scores in density of SOs in Stage 2 (r=0.47, p=.002, significant after FDR correction; Fig. 4A) and SWS (r=0.47, p=.004, significant after FDR correction; Fig. 4D), as well as SWA (r=0.32, p=.039, marginally significant after FDR correction; Fig. 4B), sigma power (r=0.3, p=.05; Fig. 4C), and the linear composite of SWA and sigma power in Stage 2 (r=0.38, p=.012, significant after FDR correction; Fig. 4F). The correlation between changes in performance and SWA in SWS was not significant (r=0.11, p=.54; Fig. 4E). Additionally, the ACE difference score for HF power in Stage 2 sleep (5-s bin *after* the peak of the Heart rate burst) was significantly correlated

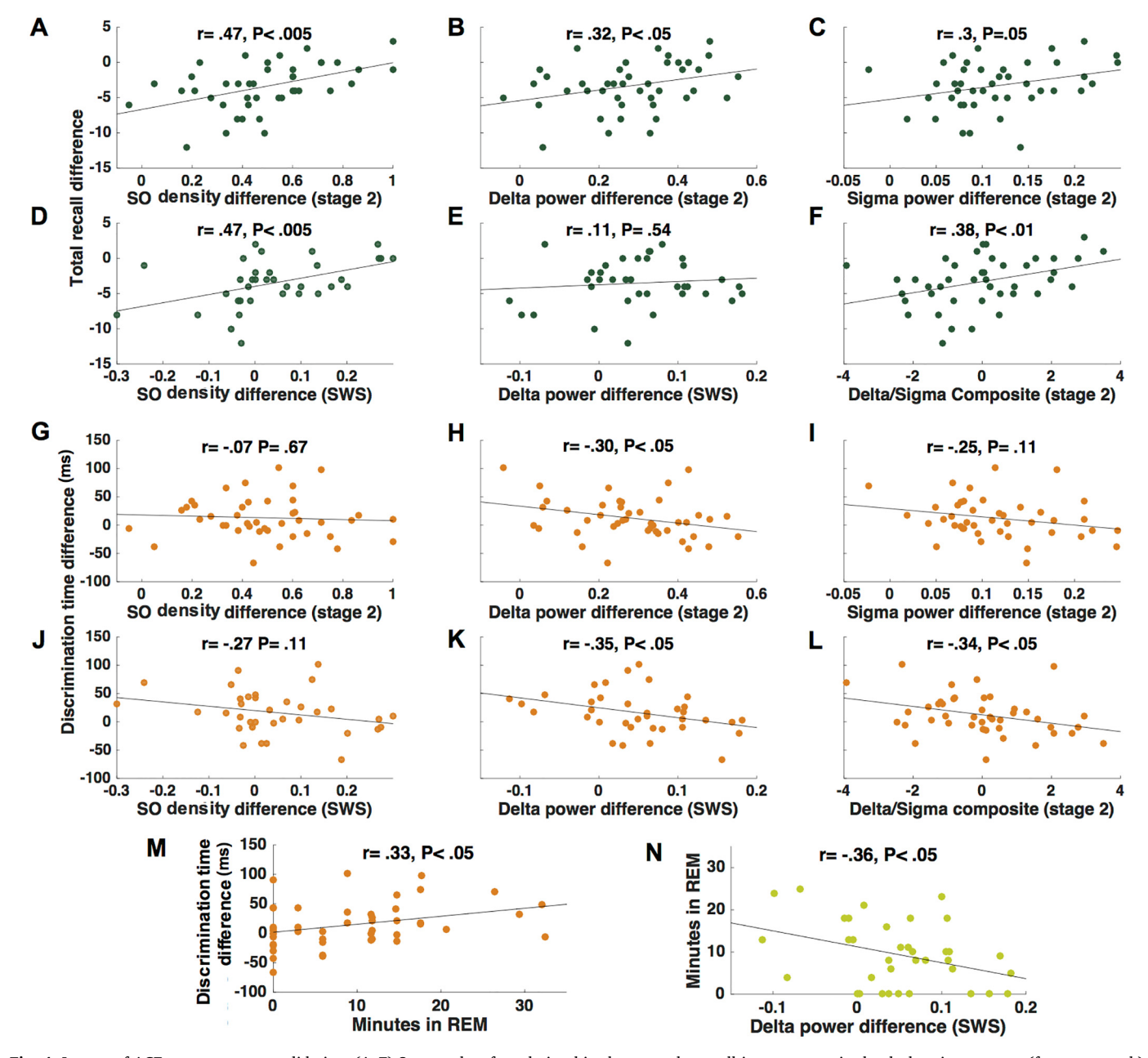


Fig. 4. Impact of ACE on memory consolidation. (A–F) Scatter plots for relationships between the recall improvement in the declarative memory (face-name task) and ACE difference scores of SO density, delta power, and sigma power during Stage 2 (n = 42) and SWS (n = 36). Note, that performance (i.e., less forgetting) was positively correlated with increase in ACE difference scores. (G–L) Scatter plots for relationships between improvement in the perceptual learning (texture discrimination task) and ACE difference scores of SO, delta power and sigma power during Stage 2 and SWS. Note, negative correlation in all cases. (M and N) Scatter plots for relationships between minutes in REM sleep and texture discrimination task learning and ACE difference scores of delta power in SWS, respectively.

with recall improvement (r = 0.32, p = .03, marginally significant after FDR correction).

To assess the relative importance for memory performance of independent autonomic and central events as well as their coupling, we utilized a hierarchical, linear regression framework. For Stage 2 and SWS, two linear regression models were calculated to predict recall difference. In Model 1, SO density, spindle density, burst density, and baseline HF power in each sleep stage were the independent variables. In Model 2, we added the ACE difference scores for SO density and spindle density *before* and HF power *after* the heart rate bursts. The regression results for Stage 2 and SWS variables are tabulated in Table 1 and Table 2, respectively. Stage 2 results showed that Model 1 was not significant ($F_{4,37} = 0.08$, $P_{4,37} = 0.08$, $P_{4,3$

 $R^2=0.23$) with both ACE SO density change and HF amplitude change as significant predictors. Comparing Model 1 and 2, we found that Model 2 explained significantly more of the variance in recall than Model 1 (change in adj $R^2=0.33$, $F_{3,34}=6.30$, p=.002). For SWS, Model 1 was not significant ($F_{4,30}=0.36$, p=.84; adj $R^2=-0.08$), but adding the ACE measures in Model 2 elevated the model to a marginal significance level ($F_{7,27}=1.53$, p=.20; adj $R^2=0.10$), with SO density change the only significant predictor. Again, Model 2 accounted for significantly more of the variance in recall improvement than Model 1 (change in adj $R^2=0.21$, $F_{3,27}=3.01$, p=.048). In summary, while the baseline HF power, SO, spindle, and Heart rate burst densities did not independently predict recall difference, ACE events predicted up to 23% of the variance in performance improvement on this declarative memory task.

Table 1
Regression models from Stage 2 variables to predict FNA total recall difference.

Variables	Model 1				Model 2			
	В	SE	t	β	В	SE	t	β
Heart rate burst density	0.39	1.84	0.21	0.04	-1.69	1.66	-1.02	-0.15
SO density	-0.13	0.40	-0.31	-0.06	-0.12	0.35	-0.35	-0.05
Spindle density	-0.16	0.90	-0.22	-0.03	0.61	0.81	0.76	0.11
Baseline HF amplitude	-5.79	26.32	-0.22	-0.04	19.98	23.53	0.85	0.13
SO density change score					6.27	2.26	2.77	0.44**
Spindle density change score					2.17	0.81	1.09	0.17
HF amplitude change score					8.56	3.46	2.47	0.38*
(Constant)	-2.83	3.32	-0.85		-8.94	3.22	-2.77	
F		0.08				2.77*		
R^2		0.01				0.36		
Adjusted R ²		-0.10				0.23		
Change in Adjusted R ²						0.33***		

^{*} p < .05.

2.4.2. Perceptual learning

We found perceptual learning was negatively related to the ACE SWA increase in Stage 2 (r=-0.30, p=.048; Fig. 4H) and SWS (r = -0.35, p = .035; Fig. 4K), as well as with the linear composite of SWA and sigma power changes in Stage 2 (r = -0.34, p = .025; Fig. 4L). In addition, non-significant negative correlations were apparent between perceptual learning and ACE SOs increases in Stage 2 (r = -0.07, p = .67; Fig. 4G) and SWS (r = -0.27, p = .11; Fig. 4J)and Stage 2 sigma power (r = -0.25, p = .11; Fig. 4I). Thus, in contrast with the positive association between ACE-mediated increases in NREM sleep events and declarative memory, perceptual learning was negatively associated with these ACE events. Given that prior studies have demonstrated the critical importance of both NREM and REM sleep for perceptual learning, the trade-off between ACE-NREM features supporting declarative memory and REM features supporting perceptual learning may not be surprising. Indeed, Fig. 4M shows a similar significant positive correlation between REM sleep and perceptual learning (r = 0.37, p = .013, marginally significant after FDR correction). We also showed a reciprocally negative correlation between ACE SWA difference score and minutes in REM (r = -0.36, p = .029; Fig. 4N). These negative associations with REM and REM-dependent learning may be related to the experimental conditions of the nap, in which subjects have a two-hour nap opportunity. Such restrictions on sleep provide boundaries on the total sleep time and may thus create a trade-off between NREM and REM sleep.

In summary, we find that sleep features associated with consolidation of hippocampal-dependent memories (SO events, SWA, and sigma power) are specifically boosted during heart rate bursts and that these ACE increases may be an important contributor in hippocampal-dependent memory consolidation. However, these benefits to declarative memory during a nap may come at the expense of REM sleep and REM-dependent perceptual learning.

2.5. Control nap

A subset of subjects (n = 22) were given a control nap one week after the experimental nap. The rationale we then employed was to test whether ACE coupling during a separate napping consolidation period was associated with individual differences in memory consolidation on the experimental day. On both experimental and control days, subjects were tested on cognitive tasks in the morning and evening and had a nap between test sessions, however, different cognitive tasks were tested on these days. This is an appropriate within-subjects control because the subjects had the same magnitude of cognitive burden, but with different information to encode, which allows us to test the specificity of the relationship between changes in the autonomic/central events during sleep and the specific memories learned. Underscoring this point, we found similar levels of Heart rate burst density (0.97 per minute) and changes in HF power (control: 20.07%, experimental: 18.61%), delta power (control: 17.65%, experimental: 21.37%), and

Table 2Regression models from SWS variables to predict FNA total recall difference.

Variables	Model 1				Model 2			
	В	SE	t	β	В	SE	t	β
Heart rate burst density	-0.43	0.55	-0.78	-0.15	-0.83	1.69	-0.49	-0.08
SO density	-0.01	0.02	-0.53	-0.10	0.03	0.08	0.42	0.07
Spindle density	-0.13	0.21	-0.62	-0.11	-0.04	0.64	-0.06	-0.01
Baseline HF amplitude	2.02	8.49	0.24	0.04	21.97	27.09	0.81	0.14
SO density change score					11.85	4.27	2.77	0.48**
Spindle density change score					0.09	1.37	0.07	0.01
HF amplitude change score					-9.11	7.38	-1.23	-0.21
(Constant)	-2.83	3.32	-0.85		-8.94	3.22	-2.77	
F		0.36				1.53		
R^2		0.05				0.28		
Adjusted R ²		-0.08				0.10		
Change in Adjusted R ²						0.18***		

^{*}p < .05.

^{**} p < .01.

^{***} p < .001.

^{**} p < .01.

^{***} p < .001.

sigma power (control: 7.64%, experimental: 8.63%) in the experimental and control naps during Stage 2 and SWS.

Next, we confirmed that these subjects had the same magnitude of effect size for the association between nap ACEs and memory on the experimental day as the entire sample. We re-ran the regression models from Table 1, in which Model 1 compared non-ACE predictors to declarative memory, and Model 2 added the ACE predictors. Indeed, a model with baseline variables did not significantly predict the declarative learning ($adj R^2 = -0.23$, p = .95), whilst adding ACE difference scores in Model 2 significantly improved the prediction ($adj R^2 = 0.47$, p = .04).

Finally, in order to confirm the specificity of the encoded material on the experimental day, correlations between control nap ACE difference scores and memory changes on the experimental day were tested. Here, evidence of no relation between the control nap ACE features and experimental memory performance would indicate a high degree of specificity to the encoded material on the experimental day. For the declarative memory task, no significant correlation was found with ACE SO density difference score in control nap Stage 2 (r = -0.04, p = .85) and SWS (r = -0.14, p = .61), as well as with the SWA changes in Stage 2 (r = 0.26, p = .24) and SWS (r = -0.35, p = .16), and sigma power changes in Stage 2 (r = 0.11, p = .63) and SWS (r = 0.14, p = .60). Unlike experimental day, there was no correlation between declarative learning and HF power change in Stage 2 (r = 0.15, p = .49). Similarly, no significant correlation was found between perceptual learning and ACE SO density increase in Stage 2 (r = 0.05, p = .82) and SWS (r = -0.18, p = .49), as well as with the SWA changes in Stage 2 (r = 0.02, p = .93) and SWS (r = 0.07, p = .78), and sigma power changes in Stage 2 (r = 0.12, p = .59) and SWS (r = 0.08, p = .75). In summary, ACE changes in the control nap were not associated with memory consolidation of information encoded on the experimental day.

3. Discussion

Here, we have identified for the first time an autonomic cardiac event (heart rate bursts) during NREM sleep that is temporally-coupled with a significant boost in central oscillations associated with systems consolidation. Specifically, we show (1) increases in the EEG amplitude in SWA and sigma bands directly preceded these large-amplitude heart rate bursts, (2) a surge in vagal activity (measured in the HF component of heart rate) directly following the Heart rate burst, (3) that the uptick in autonomic/central events (ACE) (SO, delta, sigma) and vagal activity were positively associated with declarative memory improvement and negatively associated with non-declarative memory, and (4) ACE changes in the experimental nap were only associated with memory consolidation of information encoded on the experimental day (although we note that given that the specificity of this finding is based on the absence of such associations in one control nap, further research is required with more extensive controls). Together these results present compelling evidence of a coupling between signals from the brain and heart that have a critical and specific impact on memory consolidation

Traditional calculations of EEG/ECG signals in the frequency domain using 3–5 min bins of uninterrupted nocturnal sleep have found results that differ from the present outcomes. One such study reported no association between delta power and normalized HF power at peak of SWA (Rothenberger et al., 2015). Also different from the present result, cardiac changes have been found to *precede* EEG changes by several minutes (Brandenberger et al., 2001). Here, unlike typical HRV analyses that discard large changes in HR, we intentionally analyzed all artifact-free RR intervals, which allowed for the discovery of these heart rate bursts. In addition, we used a time-domain analysis within short 20 s windows around the heart rate bursts to examine fluctuations in the EEG/ECG signals, which allowed for more fine-grained assessment of event-related changes in both signals. Similarly, using an event-related

analysis in near-infrared spectroscopy, Mensen and colleagues (Mensen, Zhang, Qi, & Khatami, 2016) reported an oscillating blood flow signal at HR frequency that was time-locked to the onset of slow waves. This study posited that the arterial pulsation evokes a down-state, or that a third generator regulating HR and slow waves may be involved. More in line with our findings, another event-based analysis revealed an increase in HR followed by a deceleration *after* spontaneous and tone-induced K-complexes (de Zambotti et al., 2016). Besides HR, other physiological responses such as pupil diameter in mice has been shown to be tightly coupled with brain activity during NREM sleep (Yüzgeç, Prsa, Zimmermann, & Huber, 2018). Pupil diameter is further known to be influenced by neuromodulator levels (Larsen & Waters, 2018) and thus suggesting a link between HR and neuromodulatory state.

By focusing on fine resolution of HR events for our event-based analysis, we found distinct bursts in HR during wake and sleep. heart rate bursts of similar duration have been identified in REM sleep in cats, with the average incidence rate of 1 burst per 6.1 min of REM sleep. These heart rate bursts were accompanied by ponto-geniculo-occipital waves and theta activity (Rowe et al., 1999), which have been associated with memory consolidation in rats (Datta, 2006). Our eventbased analyses showed SWA modulation in both Stage 2 and SWS, and sigma modulation in Stage 2 by the LF component of the RR time-series. Our results suggest that the mechanism of SWA modulation was an increase in density of SOs, and power in SWA, and sigma activity ~5 s prior to the peak of the Heart rate bursts that returned to baseline directly after the heart rate bursts. In addition, there was no significant SWA modulation in wake and REM, which is not surprising due to low SWA activity in these stages. The characteristics of the SWA and sigma modulation in NREM sleep resemble the cyclic alternating pattern (CAP) (Terzano et al., 1985) in NREM sleep which is characterized by repeated sequences of transient events and which clearly break away from the ongoing background rhythm recurring at intervals up to 1 min long. However, the average duration of SWA reactivation in CAP was reported as 12.66 s which is longer than our ACE observations. Lecci et al (Lecci et al., 2017) found periodic sigma activity (but not SWA) that was more prevalent in Stage 2 sleep than SWS and associated with memory consolidation in a declarative task (human) as well as hippocampal ripple activity (in mice). The present results, on the other hand, identified a heretofore undescribed burst in HR activity, that correlated with prominent, aperiodic, ACE-related increases in SWA and sigma, as well as parasympathetic activity, that predicted gains in declarative memory during Stage 2 and SWS. Differences between findings may be due to the focus of the Lecci paper on periodic changes in EEG activity, as opposed to using ECG as the reference point for analysis. Notwithstanding these differences in approach and outcomes, both studies point to an important link between memory consolidation and autonomic/ central events during sleep.

The present data also showed no significant correlation between heart rate bursts and traditional frequency based analysis of total LF power. This lack of relation may suggest a dissociation between mechanisms underlying LF-related sympathetic activity and heart rate bursts. In contrast, the increase in HF power directly following the heart rate bursts may instead implicate vagal inhibition (Chapleau & Sabharwal, 2011). Although specific mechanisms of ACE events are not known, we speculate that overlapping neural pathways between brain and heart centers may be an appropriate place to begin, and further investigation is needed to tease apart these mechanisms

Several candidate brainstem and cortical regions may be involved in the interaction between HR and sleep oscillations. One possibility, is that the nucleus of the solitary tract (NTS) and the rostral ventrolateral medulla (RVLM) mediate this interaction, since they act as one of the main bridges between CNS and cardiovascular systems (Guyenet, 2006). NTS is one of the critical components of the central autonomic network with afferent and efferent connections to the cardiovascular system and it receives projections from many cortical regions (van der Kooy, Koda, McGinty, Gerfen, & Bloom, 1994). Further, NTS, through

its projections to RVLMs, influences activity in the locus coeruleus (Samuels & Szabadi, 2008) and indirectly influences the basal forebrain. Indeed, increased NTS activity is associated with reduced HR, and NTS stimulation has been shown to augment EEG theta and beta power during wake in cats (Martínez-Vargas, Valdés-Cruz, Magdaleno-Madrigal, Fernández-Mas, & Almazán-Alvarado, 2016) potentially through the input to RVLM. The Heart rate burst may be a consequence of increases in spindle and slow oscillations through wide spread cortical projection to NTS (van der Kooy et al., 1994). On the other hand, one potential mechanism for SO reduction post-Heart rate burst may be via NTS projections to basal forebrain and locus coeruleus. Stimulation of these areas by the NTS increases acetylcholine and norepinephrine release in cortex, which is known to reduce slow oscillations (Krishnan et al., 2016). Taken together, this suggests that the increase of SO prior to Heart rate burst could mediate an increase of HR through combination of sympathetic and parasympathetic pathways and that the reduction of SO following Heart rate burst may arise from increased activity of NTS through parasympathetic output via the vagal nerve. However, several other pathways are known to be involved in the interaction between neocortex and heart and have be examined to make definite conclusions.

A large prior literature suggests a critical role of the ANS during wake for memory consolidation (McGaugh, 2013). Studies have found that direct modification of peripheral hormonal activity following acquisition can enhance or impair the memory storage of new information (Roozendaal & McGaugh, 2012) via vagal afferent nerve fibers, which communicate information about ANS excitation via projections to the brainstem, which then project to memory-related areas including the hippocampus, amygdala complex, and prefrontal cortex (Packard et al., 1995). Bidirectional projections from the prefrontal cortex to the hypothalamus and brainstem create a feedback loop for communication between peripheral sites and central memory areas (Thayer & Lane, 2009). Lesions of the vagus nerve impair memory (Williams & Jensen, 1993), whereas pairing vagal nerve stimulation with auditory stimuli reorganizes neural circuits, strengthens neural response to speech sounds in the auditory cortex, and enhances extinction learning of fear memories in rodents (Peña, Engineer, & McIntyre, 2013). In humans, vagal nerve stimulation enhances consolidation of verbal memory (Clark et al., 1999) and working memory (Sun et al., 2017). Recently, Whitehurst and colleagues used traditional methods to detect total sympathetic and parasympathetic power of the HRV signal during sleep and showed a correlation between parasympathetic activity during REM sleep (but not SWS) and implicit learning (Whitehurst et al., 2016). In contrast the current study used a fine-grained temporal analysis of EEG/ECG signals to reveal how the coupling of ANS/CNS Events (ACE) significantly improved the prediction of declarative memory, but not non-declarative memory, over and above total power of HR components and sleep events alone. Importantly, these effects are specific to the encoded memories directly preceding the nap. Follow-up experiments require interventions to better understand the mechanism promoting these effects, as well as probing different clinical populations that may have dampened autonomic tone during sleep, including older adults and sleep apnea. Taken together, these findings implicate a significant role of ANS modulation of plasticity and memory consolidation during sleep that is likely mediated by vagal afferents to the cortex via NTS brainstem.

4. Methods

4.1. Participants

Data reported here come from the first visit of a larger, mini-longitudinal study that included up to 7 visits per participant. Data from this study have been reported elsewhere (McDevitt et al., 2018) (Whitehurst et al., 2016) (Cellini et al., 2016) (Sattari et al., 2017). Fifty-five (30 females) healthy, non-smoking adults between the ages of 18 and 35 with no personal history of sleep disorders, neurological, psychological, or other chronic illness gave informed consent to participate in the experimental nap protocol explained below. A subset of this sample (n = 22) also participated in a one-day control nap study, whereas the other subjects did not. We therefore had the opportunity to have half the subjects tested on a different hippocampal cognitive task to match the cognitive load as the experimental day. All experimental procedures were approved by the Human Research Review Board at the University of California, Riverside and were in accordance with federal (NIH) guidelines and regulations. Participants were thoroughly screened prior to participation in the study. The Epworth Sleepiness Scale (ESS; http:// www.epworthsleepinessscale.com) and the reduced Morningness-Eveningness questionnaire (rMEO (Adan & Almirall, 1991)) were used to exclude potential participants with excessive daytime sleepiness (ESS scores > 10) or extreme chronotypes (rMEQ < 8 or > 21). Additionally, potential participants were interviewed about their medical history and quality and quantity of their sleep, including questions from the DSM-IV used to diagnose sleep-wake disorders. Participants included in the study had a regular sleep-wake schedule (reporting a habitual time in bed of about 7-9 h per night), and no presence or history of sleep, psychiatric, neurological, or cardiovascular disorders determined during screening. Participants received monetary compensation and/or course credit for participating in the study.

4.2. Data acquisition and pre-processing

4.2.1. Study procedure

Participants wore actigraphs to monitor sleep-wake activity for one week prior to the experiment to ensure participants were not sleepdeprived and spent at least 6.5 h in bed the night prior to their visit. On both the experimental and control nap days, subjects arrived at the UC Riverside Sleep and Cognition lab at 9 AM for Test Session 1. On the experimental day, cognitive tasks included a declarative and non-declarative memory task (see below), as well as a creativity measure (Whitehurst et al., 2016). On the control day, subjects were tested in a spatial navigation task and verbal memory task. The order of tasks was counterbalanced across subjects. In total, the declarative memory task took about 40 min to complete, and the non-declarative task took about 20 min to complete (the creativity measure took about 50 min, and all testing was done by approximately 11 AM). Between completing the tasks and starting the nap, participants were allowed to leave the lab and go about their normal activities, except avoiding caffeine and napping. At 12:30 PM, electrodes were attached for polysomnography (PSG) recording. At 1:30 PM, subjects took a PSG-recorded nap. They were given up to 2 h time-in-bed to obtain up to 90 min total sleep time. Sleep was monitored online by a trained sleep technician. Nap sessions were ended if the participant spent more than 30 consecutive min awake. Naps were completed at approximately 3-3:30 PM, electrodes were removed, and participants were given a break where they could leave the lab. At 5 PM, subjects returned to the lab for Test Session 2.

4.2.2. Sleep recording

Polysomnography (PSG) data including electroencephalogram (EEG), electrocardiogram (ECG), chin electromyogram (EMG), and electrooculogram (EOG) were collected using Astro-Med Grass Heritage Model 15 amplifiers with Grass GAMMA software. Scalp EEG and EOG electrodes were referenced to unlinked contralateral mastoids (F3/A2, F4/A1, C3/A2, C4/A1, P3/A2, P4/A1, O1/A2, O2/A1, LOC/A2, ROC/A1) and two submental EMG electrodes were attached under the chin and referenced to each other. ECG was recorded by using a modified Lead II Einthoven configuration. All data were digitized at 256 Hz.

4.2.3. Sleep scoring

Raw data were visually scored in 30-s epochs according to Rechtshaffen and Kales (Rechtschaffen & Kales, 1968). Wake and four sleep stages (i.e., Stage 1, Stage 2, SWS, and REM) were reclassified in

continuative and undisturbed 3-min bins and the bins were used for further analysis. The rationale of using 3-min bins was based on HRV guidelines for assessing the LF and HF components (Malik et al., 1996), as well as to have enough RR intervals to set the adaptive thresholds for heart rate burst detection.

4.2.4. Data reduction

Ten subjects were excluded from further analyses for the following reasons: (1) Four subjects did not have ECG recordings, (2) three subjects had disconnected/loose ECG reference electrodes and we were not able to detect heart beats from those subjects, (3) Three subjects had no 3-min Stage 2 and SWS epochs. Nine subjects out of the 45 subjects did not have any 3-min continuous epochs of SWS. This led to lower number of samples for SWS group. Two subjects from Stage 2 group were also considered as outliers, due to artifacts. The total number of 3-minute epochs analyzed across subjects in Wake, Stage 2, SWS, and REM were 223, 415, 275, and 147, respectively.

4.2.5. Heart-beat detection and RR time-series extraction

The ECG signals were filtered with a passband of 0.5– $100\,\mathrm{Hz}$ by Butterworth filter. R waves were identified in the ECG using the Pan-Tompkins method (Pan & Tompkins, 1985), and confirmed with visual inspection. In order to extract continuous RR tachograms, the RR intervals were resampled (at 4 Hz for power spectrum estimation; at 256 Hz for co-modulogram analysis) and interpolated by piecewise cubic spline. Zero-phase Butterworth filters were applied to the interpolated RR time-series to extract RR_{LF} and RR_{HF} .

4.2.6. Heart rate burst detection

Within 3-min bins during wake and sleep stages, the Heart rate burst events were detected as the minima in RR time-series with amplitude greater than two standard deviations below the mean of the RR time-series.

4.2.7. Power spectra

The EEG power spectrum was computed using the Welch method (4 s Hanning windows with 50% overlap). For RR time-series, the power spectral estimation was performed by the autoregressive model and the model order was set at 16.

4.3. Phase-amplitude analysis

For a given frequency pair in each stage, the RR time-series (slow or phase-providing signal) and the EEG signal (fast signal or amplitudeproviding frequency) were filtered (zero-phase infinite-impulse-response bandpass filters). Phase-providing frequencies ranged from 0.04 to 0.4 Hz (0.01 Hz increments, 0.02 Hz filter bandwidth) and amplitude-providing frequencies ranged from 0.25 to 16 Hz (0.5 Hz increments, 1 Hz filter bandwidth). The Hilbert transform was applied to the 3-min binned data. EEG amplitude and RR phase were then extracted and concatenated across the bins to construct the amplitude and phase time series, respectively. The phase time-series were binned into $36 \ 10^{\circ}$ bins (nbins = 36) and the mean of the EEG amplitude over each bin was calculated and then normalized by dividing it by the sum over the bins. Given the normalized amplitude distribution, P, the modulation index (MI) was calculated by dividing the Kullback-Leibler distance (Tort et al., 2010) of distribution P from the uniform distribution (U) by log (nbins). We then computed for each frequency pair the normalized modulation index (nMI) by generating surrogate MIs based on the method provided in supplement of (Canolty et al., 2006).

For statistical analysis, the nMIs were recalculated in 8 frequency pairs: LF (0.04–0.15 Hz)–delta (0.05–4 Hz), LF–theta (4–8 Hz), LF–alpha (8–13 Hz), LF–sigma (12–15 Hz), HF (0.15–0.4 Hz)–delta, HF–theta, HF–alpha, and HF–sigma.

The preferred phase for LF–delta modulation was calculated as angle of the average composite signal of $A_{Delta}(t)$ exp(i $\varphi_{LF}(t))$ (Canolty

et al., 2006).

4.4. Event-based analysis

4.4.1. Slow oscillation

The EEG signals of frontal and central channels were filtered (zero-phase bandpass, 0.1–4 Hz). Then, the SO were detected based on down to up-state amplitude ($>140\,\mu\text{V}$), down-state amplitude ($<-80\,\mu\text{V}$), and duration of down-state (between 0.3 and 1.5 s) and up-states (<1 s) (Dang-Vu et al., 2008).

4.4.2. Spindles

Sleep spindles were detected by applying the wavelet transform, using an 8-parameter complex Morlet wavelet with center frequency 13.5 Hz and calculating the moving average in 100 ms sliding windows. A spindle event was identified whenever the rectified signal exceeded threshold (Wamsley et al., 2012).

4.4.3. SO-spindle coupling

The SO-spindle coupling was measured by calculation of modulation index (Tort et al., 2010) between spindle activity (Morlet wavelet-filtered sigma activity (Wamsley et al., 2012)) and filtered (0.1–4 Hz) SO phase (within 2.5-s windows centered at the SO negative peak).

4.4.4. Time-locked analysis

In order to calculate changes in delta and sigma power around the Heart rate burst, the Hilbert transform was applied on filtered EEG signals in bands of interest (0.5–4 Hz for SWA and 12–15 Hz for sigma band). To assess the HF amplitude change around the Heart rate burst, the Hilbert transform was applied on $RR_{\rm HF}$.

4.4.5. Event-locked averaging

The analyses were subject-based. We first performed a within-subject average and then averaged those averages across subjects.

4.4.6. Change scores

The density of SOs (number of SOs per minute; SO negative peak was considered for counting) and spindles (spindle maximum amplitude point was considered for counting), as well as average delta and sigma amplitudes were calculated in both the 5-s window prior the heart rate bursts, as modulated values, and in periods with no Heart rate burst, as reference (baseline) values. That is, the baseline activities were calculated by excluding the 20-s periods (the segments around the heart rate bursts) from the entire stage data. For example, if we found 6 heart rate bursts during 9 min of Stage 2, the baseline Stage 2 SWA would be calculated over 7 min of non-bursting periods (9–6 * 20 s/60 s). For HF change score, the modulated values were calculated in the 5-s window after the heart rate bursts. The subtraction between modulated and reference values divided by summation of those values were calculated as the changes scores.

4.5. Statistics summary

Statistical analyses were conducted using MATLAB 2015b (MathWorks). p < .05 was considered significant.

4.5.1. Controlling the false discovery rate

In order to control for multiple comparisons, we implemented the Benjamini-Hochberg procedure of false discovery rate (FDR) correction, which compares each individual P value to its critical value, (i/m)Q, where m is the total number of comparisons, i is the P value rank, and Q=0.05 is the FDR (Benjamini & Hochberg, 1995). We reported the raw P-values, not the adjusted p-values, in the entire paper. In addition, we reported "marginally significant" when the rounded values (P values and their critical values) to two decimal places were equal.

4.5.2. Comodulogram analysis

For wake and sleep stage, the normalized modulation index (nMI) was calculated in 8 frequency pairs: LF–SWA, LF-theta, LF–alpha, LF–sigma, HF–SWA, HF–theta, HF–alpha, and HF–sigma. Within each sleep stage, the nMI pairs were compared using one-way ANOVA. The Kruskal-Wallis test was used to compare a specific nMI across sleep stages. Two-tailed unpaired-samples *t*-test was used to compare nMI of a specific frequency pair across two sleep stage.

4.5.3. Event-locked analysis

For wake and sleep stages, repeated measures ANOVAs followed by post hoc paired-samples t-tests were used to compare SWA as well as sigma activity across non-bursting periods and four 5-s bins around the heart rate bursts.

4.5.4. Test of periodicity of heart rate bursts

We calculated the inter-heart rate burst (HRB) intervals (IHBI). For a periodic system, the Poincaré map (i.e., return map) of IHBI $_{\rm n+1}$ versus IHBI $_{\rm n}$ contains one point. In a corresponding biological system with noise, this single point becomes a normally distributed single-point cluster. The Poincaré map data was considered to be a normally distributed single-point cluster if the data points along the Poincaré map axes passed a test for normality (Del Negro, Wilson, Butera, Rigatto, & Smith, 2002).

4.6. Memory performance tests

4.6.1. Face-Name association (FNA) task

Face stimuli were chosen from a UC Riverside IRB-approved database of photographs of highly diverse UC Riverside undergraduate students. All students whose photographs were included in the database provided informed consent for their picture to be used to create experimental stimuli. All faces were forward-facing, shown from the shoulders up against a plain gray background, and edited to be gray scale. First and last names were selected from the 2010 United States Census data. The five most frequent male names, female names, and last names (e.g., Smith) were eliminated. Unisex names that are commonly used for both men and women were also eliminated, as were last names that are commonly used as first names (e.g., Thomas) or contain a common first name base (e.g., Richardson). Individual face-name pairings were randomly generated for each participant so that no two participants saw the same face-name pairs. During session 1, 44 faces (22 men and 22 women) were presented in the center of the screen with a first and last name shown below the face. The first two and last two face-name pairs were discarded after encoding (i.e., not tested) due to primacy and recency effects. Each face/name pair was presented four times for duration of 4000 ms, with an inter-stimulus-interval of 500 ms. Subjects were instructed to view each face-name pair and to do their best to remember each person's name for a later test. Immediately following encoding, as well as after an 8-hr retention interval, subjects completed a recall memory test. During recall, 10 faces were presented and subjects were asked to recall the first and last names associated with each face. That is, they had the opportunity to recall 20 names (first and last names) total in each session. The ten faces tested in session 2 were different than those tested in session 1, the remaining 20 faces were used for a recognition task, and those results are reported elsewhere (Sattari et al., 2017). Total recall was calculated as the sum of first and last names recalled correctly. The difference in total recall between sessions (PM-AM) was calculated as a measure of declarative memory consolidation.

4.6.2. Texture discrimination task (TDT)

Subjects performed a texture discrimination task similar to that developed by Karni & Sagi (Karni & Sagi, 1991). Visual stimuli for the TDT were created using the Psychophysics Toolbox (Brainard, 1997). Each stimulus contained two targets: a central letter ('T' or 'L'), and a

peripheral line array (vertical or horizontal orientation) in one of four quadrants (lower left, lower right, upper left, or upper right) at 2.5°–5.9° eccentricity from the center of the screen. The quadrant was counterbalanced across subjects. The peripheral array consisted of three diagonal bars that were either arranged in a horizontal or vertical array against a background of horizontally oriented background distracters, which created a texture difference between the target and the background.

An experimental *trial* consisted of the following sequence of four screens: central fixation cross, target screen for 33 ms, blank screen for a duration between 0 and 600 ms (the inter-stimulus-interval, or ISI), mask for 17 ms, followed by the response time interval (2000 ms) and feedback (250 ms, red fixation cross with auditory beep for incorrect trials and green fixation cross for correct trials) before the next trial. Subjects discriminated two targets per trial by reporting both the letter at central fixation ('T' or 'L') and the orientation of the peripheral array of three diagonal lines (horizontal or vertical) by making two key presses. The central task controlled for eye movements.

Each block consisted of 25 trials, each with the same ISI. A threshold was determined from the performance across 13 blocks, with a progressively shorter ISI, starting with 600 ms and ending with 0 ms. The specific sequence of ISIs across an entire session was (600, 500, 400, 300, 250, 200, 167, 150, 133, 100, 67, 33, 0). A psychometric function of percent correct for each block was fit with a Weibull function to determine the ISI at which performance yielded 80% accuracy. TDT performance was calculated as the difference in threshold between Session 1 and Session 2, such that a positive score indicates performance improvement (i.e., decreased threshold in Session 2), whereas a negative score indicates deterioration.

Subjects were given task instructions and practiced the task during an orientation appointment prior to starting the study. During this practice, the peripheral target was located in a quadrant that was not used during the study. This practice ensured that subjects understood the task and accomplished the general task learning that typically occurs the first time a subject performs a task. Additionally, on the study day, subjects were allowed to practice an easy version of the task (ISI of 1000–600 ms) prior to starting the test session to make sure subjects were able to discriminate the peripheral target between 90% and 100% correct on an easy version of the task.

Acknowledgement

This work was supported by grants from NIH (R01AG046646), ONR (MURI: N000141310672), NSF (IIS-1724405), and Young Investigator Prize to Sara C. Mednick. MN would like to thank Nicola Cellini and Lauren N. Whitehurst for their skillful help in statistical analysis and data interpretation. Maryam Ahmadi, Negin Sattari, Benjamin D Yetton are thanked for reading through drafts of the manuscript. The authors declare no conflict of interest.

Author contributions

Conceived and designed the experiments: SCM EAM. Performed the experiments: SCM EAM. Analyzed the data: MN GPK EAM. Wrote the paper: MN GPK MB SCM.

Appendix A. Supplementary material

Supplementary data to this article can be found online at https://doi.org/10.1016/j.nlm.2018.12.008.

References

Adan, A., & Almirall, H. (1991). Horne and östberg morningness-eveningness questionnaire: A reduced scale. *Personality and Individual Differences, 12*(3), 241–253. Arbon, E. L., Knurowska, M., & Dijk, D. J. (2015). Randomised clinical trial of the effects

- of prolonged-release melatonin, temazepam and zolpidem on slow-wave activity during sleep in healthy people. *Journal of Psychopharmacology*, 29(7), 764–776.
- Benjamini, Y., & Hochberg, Y. (1995). Controlling the false discovery rate: A practical and powerful approach to multiple testing. *Journal of the Royal Statistical Society. Series B* (Methodological), 57(1), 289–300.
- Billman, G. E. (2013). The LF/HF ratio does not accurately measure cardiac sympathovagal balance. Frontiers in Physiology, 4, 1–5.
- Brainard, D. H. (1997). The psychophysics toolbox. *Spatial Vision*, 10(4), 433–436. Brandenberger, G., Ehrhart, J., Piquard, F., & Simon, C. (2001). Inverse coupling between
- ultradian oscillations in delta wave activity and heart rate variability during sleep.

 Clinical Neurophysiology, 112(6), 992–996.
- Canolty, R. T., Edward, E., Dalal, S. S., Soltani, M., Nagarajan, S. S., Kirsch, H. E., ... Knight, R. T. (2006). High gamma power is phase-locked to theta oscillations in human neocortex. *Science*, 313(5793), 1626–1628.
- Cellini, N., Whitehurst, N. L., McDevitt, E. A., & Mednick, S. C. (2016). Heart rate variability during daytime naps in healthy adults: Autonomic profile and short-term reliability. *Psychophysiology*, 53(4), 473–481.
- Chapleau, M. W., & Sabharwal, R. (2011). Methods of assessing vagus nerve activity and reflexes. Heart Failure Reviews, 16(2), 109–127.
- Clark, K. B., Naritoku, D. K., Smith, D. C., Browning, R. A., & Jensen, R. A. (1999). Enhanced recognition memory following vagus nerve stimulation in human subjects. *Nature Neuroscience*, 2(1), 94–98.
- Dang-Vu, T. T., Schabus, M., Desseilles, M., Albouy, G., Boly, M., Darsaud, A., ... Maquet, P. (2008). Spontaneous neural activity during human slow wave sleep. *Proceeding of National Academy of Sciences*, 105(39), 15160–15165.
- Datta, S. (2006). Activation of phasic pontine-wave generator: A mechanism for sleepdependent memory processing. Sleep and Biological Rhythms, 4, 16–26.
- de Zambotti, M., Willoughby, A. R., Franzen, P. L., Clark, D. B., Baker, F. C., & Colrain, I. M. (2016). K-complexes: interaction between the central and autonomic nervous systems during sleep. Sleep, 39(5), 1129–1137.
- Del Negro, C. A., Wilson, C. G., Butera, R. J., Rigatto, H., & Smith, J. C. (2002). Periodicity, mixed-mode oscillations, and quasiperiodicity in a rhythm-generating neural network. *Biophysical Journal*, 82(1 Pt 1), 206–214.
- Fruhistorfer, H., Partanen, J., & Lumio, J. (1971). Vertex sharp waves and heart action during the onset of sleep. *Electroencephalography and Clinical Neurophysiology*, 31(6), 614–617.
- Gais, S., & Born, J. (2004). Declarative memory consolidation: Mechanisms acting during human sleep. *Learning and Memory*, 11, 679–685.
- Guyenet, P. G. (2006). The sympathetic control of blood pressure. Nature Reviews Neuroscience. 7, 335–346.
- Hall, S. D., Prokic, E. J., McAllister, C. J., Ronnqvist, K. C., Williams, A. C., Yamawaki, N., ... Stanford, I. M. (2014). GABA-mediated changes in inter-hemispheric beta frequency activity in early-stage Parkinson's disease. *Neuroscience*, 5(281), 68–76.
- Karni, A., & Sagi, D. (1991). Where practice makes perfect in texture discrimination: Evidence for primary visual cortex plasticity. Proceedings of the National Academy of Sciences USA, 88, 4966–4970.
- Krishnan, G. P., Chauvette, S., Shamie, I., Soltani, S., Timofeev, I., Cash, S. S., ... Bazhenov, M. (2016). Cellular and neurochemical basis of sleep stages in the thalamocortical network. *eLife*, 5(e18607).
- Larsen, R. S., & Waters, J. (2018). Neuromodulatory correlates of pupil dilation. Frontiers in Neural Circuits, 12(21).
- Lecci, S., Fernandez, M. L., Weber, F. D., Cardis, R., Chatton, J.-Y., Born, J., & Lüthi, A. (2017). Coordinated infraslow neural and cardiac oscillations mark fragility and offline periods in mammalian sleep. Science Advances, 3(e1602026), 1–14.
- Lechinger, J., Heib, D. P., Gruber, W., Schabus, M., & Klimesch, W. (2015). Heartbeat-related EEG amplitude and phase modulations from wakefulness to deep sleep: Interactions with sleep spindles and slow oscillations. *Psychophysiology*, 52(11), 1441–1450.
- Malik, M., Camm, A. J., Bigger, J. T., Breithardt, G., Cerutti, S., Cohen, R. J., ... Singer, D. H. (1996). Heart rate variability. Standards of measurement, physiological interpretation, and clinical use. *European Heart Journal*, 17(3), 354–381.
- Martínez-Vargas, D., Valdés-Cruz, A., Magdaleno-Madrigal, V. M., Fernández-Mas, R., & Almazán-Alvarado, S. (2016). Effect of electrical stimulation of the nucleus of the solitary tract on electroencephalographic spectral power and the sleep-wake cycle in freely moving cats. *Brain Stimulation*, 10(1), 116–125.
- McDevitt, E. A., Sattari, N., Duggan, K. A., Cellini, N., Whitehurst, L. N., Perera, C., ... Mednick, S. C. (2018). The impact of frequent napping and nap practice on sleep-dependent memory in humans. *Scientific Reports*, 8, 15053.
- McGaugh, J. L. (2013). Making lasting memories: Remembering the significant. Proceedings of the National Academy of Sciences of the United States of America, 110(Suppl 2), 10402–10407.
- Mednick, S. C., McDevitt, E., Walsh, J. K., Wamsley, E., Paulus, M., Kanady, J. C., & Drummond, S. P. (2013). The critical role of sleep spindles in hippocampal-dependent memory: A pharmacology study. *The Journal of Neuroscience*, 33(10), 4494–4504.
- Mensen, A., Zhang, Z., Qi, M., & Khatami, R. (2016). The occurrence of individual slow

- waves in sleep is predicted by heart rate. Scientific Reports, 6, 29671.
- Mölle, M., Eschenko, O., Gais, S., Sara, S. J., & Born, J. (2009). The influence of learning on sleep slow oscillations and associated spindles and ripples in humans and rats. *European Journal of Neuroscience*, 29(5), 1071–1081.
- Niknazar, M., Krishnan, G. P., Bazhenov, M., & Mednick, S. C. (2015). Coupling of Thalamocortical Sleep Oscillations Are Important for Memory Consolidation in Humans. Plos One, 10(12), e0144720.
- Norton, K. N., Luchyshyn, T. A., & Shoemaker, J. (2013). Evidence for a medial prefrontal cortex–hippocampal axis associated with heart rate control in conscious humans. *Brain Research*, 104–105.
- Packard, M. G., Williams, C. L., Cahill, L., & McGaugh, J. L. (1995). The anatomy of a memory modulatory system: From periphery to brain. In N. E. Spear, L. P. Spear, & M. L. Woodruff (Eds.). Neurobehavioral plasticity: Learning, development and response to brain insults (pp. 149–184). New Jersey: Lawrence Erlbaum Associates.
- Pan, J., & Tompkins, W. J. (1985). A real-time QRS detection algorithm. IEEE Transactions on Biomedical Engineering, 32(3), 230–236.
- Pedemonte, M., Goldstein-Daruech, N., & Velluti, R. A. (2003). Temporal correlations between heart rate, medullary units and hippocampal theta rhythm in anesthetized, sleeping and awake guinea pigs. *Autonomic Neuroscience: Basic and Clinical*, 107(2), 99–104.
- Peña, D. F., Engineer, N. D., & McIntyre, C. K. (2013). Rapid remission of conditioned fear ex- pression with extinction training paired with vagus nerve stimulation. *Biological Psychiatry*, 73(11), 1071–1077.
- Rechtschaffen, A., & Kales, A. (1968). A manual of standardized terminology, techniques and scoring system for sleep stages of human subjects. Los Angeles: Brain Information Services/Brain Research Institue, University of California.
- Roozendaal, B., & McGaugh, J. L. (2012). Memory modulation. *Behavioral Neuroscience*, 125(6), 797–824.
- Rothenberger, S. D., Krafty, R. T., Taylor, B. J., Cribbet, M. R., Thayer, J. F., Buysse, D. J., ... Hall, M. H. (2015). Time-varying correlations between delta EEG power and heart rate variability in midlife women: The SWAN Sleep Study. *Psychophysiology*, 52(4), 572–584.
- Rowe, K., Moreno, R., Lau, T., Wallooppillai, U., Nearing, B. D., Kocsis, B., ... Verrier, R. L. (1999). Heart rate surges during REM sleep are associated with theta rhythm and PGO activity in cats. *American Journal of Physiology*, 277(3), R843–R849.
- Samuels, E. R., & Szabadi, E. (2008). Functional neuroanatomy of the noradrenergic locus coeruleus: Its roles in the regulation of arousal and autonomic function part I: Principles of functional organisation. *Current Neuropharmacology*, 6(3), 235–253.
- Sattari, N., McDevitt, E. A., Panas, D., Niknazar, M., Ahmadi, M., Naji, M., ... Mednick, S. C. (2017). The effect of sex and menstrual phase on memory formation during a nap. Neurobiology of Learning and Memory, 145, 119–128.
- Staresina, B. P., Bergmann, T. O., Bonnefond, M., van der Meij, R., Jensen, O., Deuker, L., ... Fell, J. (2015). Hierarchical nesting of slow oscillations, spindles and ripples in the human hippocampus during sleep. *Nature Neuroscience*, 18, 1679–1686.
- Sun, L., Peräkylä, J., Holm, K., Haapasalo, J., Lehtimäki, K., Ogawa, K. H., ... Hartikainen, K. M. (2017). Vagus nerve stimulation improves working memory performance. Journal of Clinical and Experimental Neuropsychology, 1–11.
- Terzano, M. G., Mancia, D., Salati, M. R., Costani, G., Decembrino, A., & Parrino, L. (1985). The cyclic alternating pattern as a physiologic component of normal NREM sleep. Sleep, 8(2), 137–145.
- Thayer, J. F., & Lane, R. D. (2009). Claude Bernard and the heart-brain connection: Further elaboration of a model of neurovisceral integration. *Neuroscience and Biobehavioral Reviews*, 33(2), 81–88.
- Tort, A. B., Komorowski, R., Eichenbaum, H., & Kopell, N. (2010). Measuring phaseamplitude coupling between neuronal oscillations of different frequencies. *Journal of Neurophysiology*, 104(2), 1195–1210.
- van der Kooy, D., Koda, L. Y., McGinty, J. F., Gerfen, C. R., & Bloom, F. E. (1994). The organization of projections from the cortex, amygdala, and hypothalamus to the nucleus of the solitary tract in rat. *The Journal of Comparative Neurology*, 224(1), 1–24.
- Vanoli, E., Adamson, P. B., Ba-Lin, Pinna, G. D., Lazzara, R., & Orr, W. C. (1995). Heart rate variability during specific sleep stages. A comparison of healthy subjects with patients after myocardial infarction. *Circulation*, 91(7), 1918–1922.
- Wamsley, E. J., Tucker, M. A., Shinn, A. K., Ono, K. E., McKinley, S. K., Ely, A. V., ... Manoach, D. S. (2012). Reduced sleep spindles and spindle coherence in schizophrenia: mechanisms of impaired memory consolidation? *Biological Psychiatry*, 71(2), 154-161
- Whitehurst, L. N., Cellini, N., McDevitt, E. A., Duggan, K. A., & Mednick, S. C. (2016). Autonomic activity during sleep predicts memory consolidation in humans. Proceedings of National Academy of Science, 113(26), 7272–7277.
- Williams, C. L., & Jensen, R. A. (1993). Effects of vagotomy on Leu-enkephalin-induced changes in memory storage processes. *Physiology & Behavior*, *54*(4), 650–663.
- Yüzgeç, Ö., Prsa, M., Zimmermann, R., & Huber, D. (2018). Pupil size coupling to cortical states protects the stability of deep sleep via parasympathetic modulation. *Current Biology*, 28, 392–400.